EMBEDDED SENSOR NETWORK DESIGN FOR SPATIAL SNOWCOVER

Robert Rice[1] and Roger Bales[1]

ABSTRACT

Scaling point observations of snow water equivalent (SWE) to model grid-element scales is particularly challenging given the considerable sub-grid variability in snow accumulation over complex terrain. In an effort to capture this sub-grid variability and provide spatially explicit ground-truth snow data an embedded snow sensor network was designed and installed in Yosemite National Park. Extensive snow surveys were used to guide the installation of the network and to relate the observations to more detailed spatial SWE fields. Four years of continuous spatial and temporal data from both Yosemite National Park indicate that accumulation and ablation rates can vary as much as 50% based on variability in topography and vegetation. These snow distribution patterns are especially apparent in the open forests where vegetation structure largely controls variability in snow distribution. Comparisons with historical snow course data shows that a single point measurement is a poor estimator of snow depth over a homogenous area, but 4 or more measurement points can reduce the uncertainty by 50%. Further analyses indicated that an optimal snow depth network consists of 7 to 10 snow depth sensors. These spatial and temporal measurement arrays will improve remotely sensed and modeled SWE estimates by providing robust, spatially explicit ground-truth values of snowpack states.

INTRODUCTION

Ground-based observations of snow have long supported operational water resource management, yet historical point measurements leave montane catchments under-sampled both spatially and temporally. Estimation of both physical processes and snow-related quantities are subject to considerable uncertainty in mountainous regions because of sub-grid variability. Advances in ground based measurements are being outpaced by remote sensing and modeling, and strategic intensification of in-situ measurements will provide the means to reduce uncertainty in estimates of hydrologic fluxes and processes (Bales et al., 2006).

The spatial distribution of snow, expressed as snow water equivalent (SWE), is a particularly important state variable given that snow provides the majority of the water input to the mountains of the Western U.S. and dramatically influences energy exchange between the land surface and the atmosphere. The ideal spatial resolution for estimating SWE is one that reduces sub-grid element heterogeneity to a level where most of the variability in the system can be modeled explicitly (Blöschl, 1999). SWE is measured at over 1,700 real-time snow sensor stations and manual snow courses in the western United States, from a combination of monthly manual snow surveys and continuous telemetered snow pillows. While these points provide regional knowledge of snow amounts, they are insufficient to resolve the spatial variability of snow at the basin scale.

In most of the Sierra Nevada, the California Cooperative Snow Survey coordinates measurement programs, while the Natural Resource Conservation Service manages the snow telemetry (SNOTEL) network across the rest of the West. Snow sensors and snow courses support forecasts of seasonal runoff volumes using empirical relationships between point values of SWE, antecedent soil moisture, historical temperature and precipitation data, and observed runoff. Snow courses were placed in areas that are representative of the water producing regions of a watershed, in order to provide indices of streamflow. Many snow courses were installed in the 1930's, with others later, using relatively empirical methods of site selection, with the main criteria being site accessibility and protection from public disturbance. Locations are characterized by a homogenous snow cover, and snow courses are on flat or nearly flat ground. Moreover, they must be accessible during winter without exposing the surveyors to avalanche danger. Though the manual snow courses provide many long time series, and the snow telemetry stations provide daily or even hourly temporal resolution, the spatial resolution is sparse. Their locations do not represent the range of physiographic condition found within the catchments in which they are located (Dressler et al., 2006). Therefore snow courses and automated snow stations were not designed to provide SWE values that are representative of the average values within a grid element. Nevertheless, the network has been used to estimate the

---

Paper presented Western Snow Conference 2008

[1] Sierra Nevada Research Institute, University of California, Merced, P.O. Box 2039, Merced, CA 95344, rrice@ucmerced.edu.

spatial distribution of SWE (Molotch et al., 2004; Fassnacht et al., 2003; Daly et al., 2000, Carroll and Cressie, 1996; Ling, et al., 1995; Carroll et al., 1993) and to update snowpack model state variables within data assimilation schemes (Brubaker and Menoes, 2001; Carroll et al., 2001; Shafer et al, 1979). The use of snow measurement network data in these applications implicitly assumes that the SWE values are representative of the grid elements encompassing them Precipitation and snow accumulation in the western U.S. varies spatially and temporally because of topography—elevation, orientation, vegetation—and larger-scale synoptic processes. Therefore, substantial variations exist between snow measurements, even from sites in close proximity (Carroll et al., 1999). McGurk et al. (1993) analyzed relationships between low- and high-elevation snow courses and found the correlations unreliable because the early disappearance of snow at the lower elevations gives no further information about snow at the higher elevations. Another consequence of the current snowpack sampling and empirical/statistical runoff forecasting strategy is errors that would result from different precipitation distribution which are not known. Current forecasts in the Sierra Nevada and across the West do well for mean conditions, but poorly at the extremes (Franz et al., 2003). Current methods perform poorly for conditions not well represented in the historical record. Conditions are likely to be further from the historical mean given observed and projected changes in snowpack and hydrologic processes (Cayan, 1996; Mote et al., 2005; Stewart et al., 2005.). Further, given these changes in climate, water management can no longer be business as usual, as predicted changes in streamflow runoff will push these statistical runoff models beyond the range of historical behavior (Milley et al., 2008).

Three questions are addressed in this research: First, are monthly snow course measurements, specifically the 10 spatially distributed sampling points that comprise the monthly mean SWE, representative of the variability of the surrounding terrain? Second, can a distributed, embedded sensor network be designed and installed in optimal locations, based on extensive snow surveys, in order to capture of the complex snow distribution patterns driven by the physiographic features during the accumulation and ablation periods? Third, are the snow depth observations within a dense cluster of snow depth measurements indicative of the spatial mean and variability of snow within grid elements of various spatial resolutions?

STUDY AREA

Yosemite National Park

This study was conducted at Gin Flat (37°46'0.93"N, 119°46'26"W) at an elevation of 2,100-m in the Upper Merced River Basin located in the Sierra Nevada of California. Gin Flat is also the location of a snow course (1930-present) and snow sensor (1980-present) sites operated by the California Department of Water Resources (CDWR) (Figure 1). Gin Flat was chosen because of its long term data sets, ease of access, and variable terrain. The distributed snow measurement network was deployed across a mixed conifer 0.4-ha plot where tree canopy densities of >60% influence snow distribution patterns. Since this study site was located in Yosemite National Park our installation of the embedded sensor network was limited to the 122-m wide non-wilderness corridor centered on Tioga Pass Road. However, snow surveys were conducted over a 4 km^2 area surrounding Gin Flat, and included both non-wilderness and wilderness areas.

METHODS

Two approaches were used to estimate the spatial variability of snow. The first examines the historical snow course records, involving 10 point measurements with a Mt. Rose Sampler along a 300-m transect, from the snow survey field notes dating back to 1930. Only the averages of these 10 snow depth measurements are generally reported by the snow survey cooperatives. The 10 individual depths were examined for all 14 snow courses located in Yosemite National Park. The second approach used an embedded sensor network consisted of 10 ultra-sonic snow depth sensors that are strategically located based on the physiographic features within the 0.4 ha area. To verify that the embedded sensor network was capturing the spatial variability of snow depth, and evaluate its ability to estimate the spatial mean, extensive snow surveys were performed within a 1- and 4-km^2 grid and coupled with a binary regression tree analysis identified the independent physiographic variables (e.g. elevation, solar radiance, slope, aspect, vegetation density) that control the distribution of snow depth and provide the basis for the interpolation of snow depth to a 20-m grid. (Molotch and Bales, 2005).

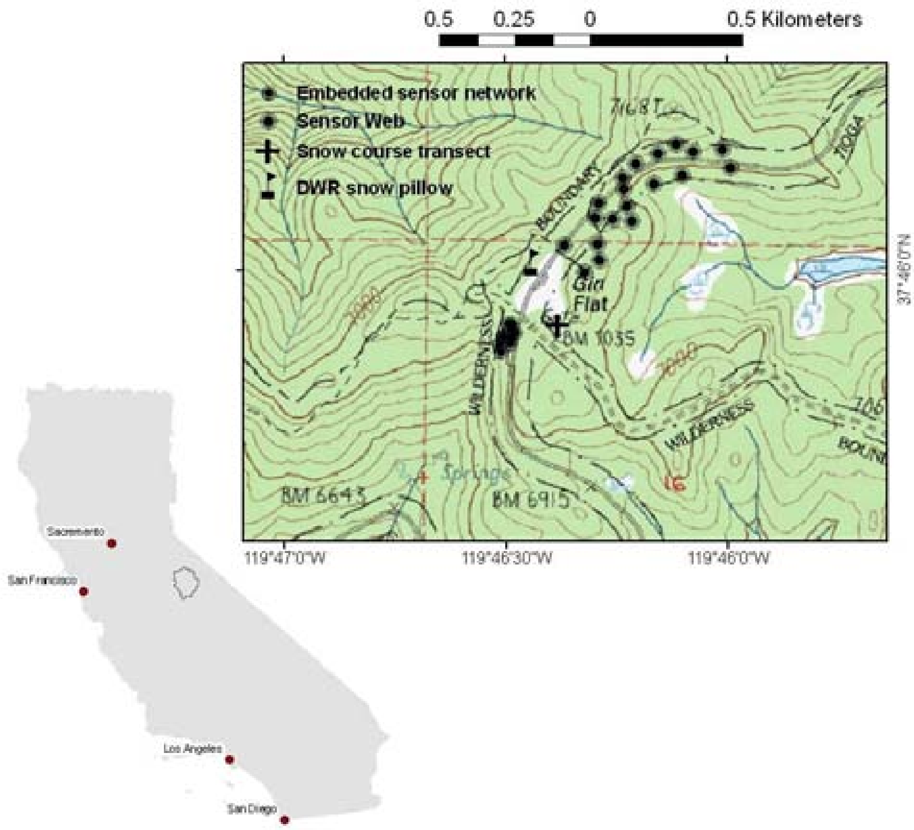

Figure 1. Gin Flat study area located in Yosemite National Park.

Historical Snow Course Data

Historical snow course field notes, for 1930-1997, were obtained from CDWR and manually digitized. Each snow course is situated below timberline on flat or nearly flat terrain, and characterized by homogenous snow cover and snowpack conditions. Prior to 1950, snow courses sampled 15-20 points, but were reduced to 10 points as the additional 5 points did not decrease the uncertainty of capturing the spatial mean. Snow courses in Yosemite National Park are surveyed by National Park Service personnel using a Federal snow sampler near the first of each month beginning in January and extending to as late as May, depending on snow conditions.

Embedded Sensor Network

In an effort to capture this sub-grid variability and provide spatially explicit ground-truth snow data an embedded snow sensor network was designed and installed at Gin Flat in Yosemite National Park. Extensive snow surveys were used to guide the installation of the network and to relate the observations to more detailed spatial SWE fields. Four years of continuous spatial and temporal data from Yosemite indicate that accumulation and ablation rates can vary as much as 50% based on variability in topography and vegetation. These snow distribution patterns are especially apparent in the open forests where vegetation structure largely controls variability in snow distribution.

An embedded sensor network consisting of 10 ultra-sonic snow depth sensors (e.g. Judd Communications) was deployed in November 2003. The depth sensors were installed atop a 3-m steel mast, extending outward 0.61-m from the top, and logged snow depth and air temperature hourly. The mast was bolted to a U-post that was driven 0.6-m into the ground. The stake provides stability and added strength for snow creep and glide.

Ten depth sensors were placed strategically throughout the 0.4 ha site which had variable: slope, aspect, vegetation and elevation. A centrally located datalogger (Campbell Scientific CR10x) with 12-volt photovoltaic power supply was housed in a weather proof enclosure and mounted to the 3-m mast. Wires extended from this central point too the sensors, to a maximum distance of 55-m. Beyond 55-m, resistance in the wire created signal loss.

Field Surveys

To evaluate the representativeness of the embedded sensor network, snow surveys were performed in 2006 during both accumulation and ablation periods. A binary regression tree model, physiographic variables, and detailed observations of snow depth where used to model the distribution of snow depth at three scales (i.e. 1, 4, and 16 km^2) around the snow sensors.

Field surveys of snow depth and density were performed on February 7-10 to correspond with the accumulation period, and again on April 4-7 to correspond with the ablation period. Snow surveys were conducted in a 1- and 4-km^2 study area, with both sampling grids centered on the snow sensor at Gin Flat. A total of 144 snow depth points were measured and 8 snow pits were dug and sampled for density. In the 1-km^2 study area 80 sample points extending in the cardinal directions were sampled, at 25-m measurement intervals; while in the 4-km^2 area 64 sample points were sampled with a 250-m measurement interval. Snow density was measured at 4 locations within the 1- and 4-km^2 grid. Snow pits were excavated and snow density was measured at 10-cm vertical intervals using a 1,000 cm^3 stainless steel snow cutter. Snow samples were weighed using a digital scale with a 1 g resolution.

Locations of the 144 points were defined in ARCGIS®, and stored in a handheld computer equipped with a Global Positioning System (GPS) receiver and GIS software. On the handheld unit, the 144 points were overlaid on a USGS 7.5-minute topographical map. The GPS unit was used to navigate to the sample points where snow depth was recorded. At each sample point, 4 depth measurements were taken and recorded, 5-m around the central point. The 4 sample points were averaged, and their mean was considered representative of snow depth.

Physiographic Parameters

Elevation, slope, and aspect were from a 10-m U.S. Geological Survey digital elevation model (DEM) derived from the standard level 1 7.5-minute topographic map series provided by the Yosemite National Park. The initial DEM was cast to the Universal Transverse Mercator (UTM) projection system and is referenced to the North American Datum (NAD) of 1927 (NAD27). This projection was chosen because it respects the cardinal directions (extending from the center of the projections). The DEM was then up-scaled to a 20-m resolution resulting in 40,000 records for the 16-km^2 area.

A solar radiation index was calculated using the TOPQUAD algorithm (Dozier, 1980) using clear sky conditions. The method used here was to calculate the daily radiation for the fifteenth day of each month on the 20-m grid, then calculate the mean to yield a solar radiation index. For the February snow survey, the daily cumulative solar radiation was calculated for the 15th of each month for November to January, and averaged across the 3-month period. The April snow survey, the daily cumulative solar radiation was calculated and averaged from November to March.

The vegetation density was deduced from a vegetation index based on aerial photography (personnel communication, Jan Van Wagtendonk, USGS). The vegetation indices range in value from 1 to 6 representing the canopy density. The vegetation density is preferred to the vegetation index for observations and linear regression analysis.

Binary Regression Tree

Binary regression tree analysis was used to identify the independent physiographic variables (e.g. elevation, solar radiance, slope, aspect, vegetation density) that affect the distribution of snow depth and SWE and provided the basis for the interpolation of snow depth across the grids (Molotch et al., 2004).

Optimal locations were found by identifying the lowest deviances for each 20-m pixel from the mean of the modeled snow depth. Areas with the lowest deviance were identified as the optimal locations for a measurement network (Molotch and Bales, 2005). SWE was not used for defining optimal site locations given the higher uncertainty in the distributed SWE estimates than the distributed snow depth measurements, as well as the capability of the embedded network measuring only snow depth.

RESULTS

Historical Snow Course Analysis

There was considerable homogeneity in snow depth across each of the 14 snow courses, but variability in the spatial mean does exist on both an inter-seasonal and inter-annual basis, indicating variations in seasonal and annual climate and across elevations. To examine the source of this within-snow-course variability within each snow course record, the historical mean for each individual sample point was computed along, with the CV. As the mean April 1 snow depth declines for each sample point the CV increases, especially at most of the points within the lower elevation sites (e.g. Beehive Meadow and Vernon Lakes), showing a higher degree of variability than the high-elevation snow courses, with CV's reaching 0.7 (Figure 2).

Field Surveys

The February 7-10 survey at Gin Flat was during a 3-week period with unseasonably warm temperatures. By March 1 the snow courses across the Sierra Nevada showed the snowpack to be 85% of the historical average, with the Upper Merced River Basin was 75% of normal. Thus, the results of the February survey were actually characteristic of an ablation period. The average snow depth across both the 1- and 4-km^2 sampling grid was 67-cm, with a mean density of 384 kg.m^{-3}. The second survey at Gin Flat occurred on April 4-7. There was a rain-on-snow event up to 2,300-m on April 4; while on April 5, 50-cm of high-density snow fell and the survey was cancelled because of falling trees. The following two days provided stable weather conditions, but warm temperatures and the melting fresh snow, provided difficult travel conditions; hence, 16 depth measurements in the northern section on the grid could not be surveyed. Thus 129 snow depth measurements were taken, and 6 snow pits were sampled for density. The average snow depth was 187 cm with an average density of 315 kg m^{-3}. Despite the rain on April 4, the significant March snowfall provided an above average snowpack with the Sierra Nevada at 125% of the historical average, while the Upper Merced River Basin was 124% of normal. Therefore, the April snow survey was considered indicative of the accumulation period. A CV of 0.40 was reported for the February survey for both the 1- and 4-km^2 study area. In April the respective CV's were 0.20 and 0.27.

Binary Regression Tree Analysis

The relationship between snow depth and the physiographic variables differed between the February and April snow surveys at Gin Flat. In February, which was characterized by unseasonably warm temperatures, vegetation density, slope, and aspect played the dominant roles in the distribution patterns, with the deeper snow depths being in open areas, on either flat terrain or north-facing slopes. The prediction tree had fifteen terminal nodes and explained 60% of the initial variance. Residuals were normally distributed, with a standard deviation of 17-cm. In April, which was characteristic of the accumulation season, elevation, vegetation density, and solar radiation were dominant as deeper snow depths resulted from orographic enhancement, areas with low canopy density, and lower solar irradiance, resulting from cloud cover. The prediction tree had ten terminal nodes, and explained 55% of the initial variance. The residuals were normally distributed, with a standard deviation of 29-cm. Modeled snow depths across the 1-, 4-, and 16-km^2 landscape surrounding Gin Flat were similar for all 3 scales, with a minimum of 38 cm, a maximum of 116 cm, and a mean across the 1-, 4-, and 16-km^2 area of 69-, 64-, and 62-cm, respectively (Figure 3). CV's were also relatively similar across the 1-, 4-, and 16-Km^2 modeled areas, at 0.30 for February and 0.18 for April. The higher CV's are for the ablation period, while the lower CV's are indicative for the accumulation period. One might expect the snow variability to increase as the modeled area increases, but at Gin Flat, the distribution of independent variables, which control snow distribution patterns are equally representative across the 1-, 4-, and 16-km^2. Slightly higher snow depths were modeled at 1–km^2, as this area has slightly lower vegetation density, with only 45% of the area covered by canopy density's of >60%, as well as only 5% of its terrain having a southwest aspect compared to 15% for the 4- and 16-km^2, 25% of the terrain has a Northwest aspect, thus providing for slightly higher accumulated snow depths. This is also apparent when examining Figure 3, in which the mean depth within the 1–km^2 grid elements is slightly higher, as much as 10%, than that in both the 4– and 16–km^2 areas, as elevation is an important component in the latter.

Embedded Sensor Network.

Snow depth across the distributed network varied as much as 50% (Figure 4), with tree canopy density of >60% influencing distribution patterns the most. The Gin Flat snow pillow and snow course was at least 25% higher than the sensor network mean. Further, the 10 point measurements within the snow course, placed in relatively homogenous, flat, open terrain, are not good indicators of either the spatial average, or the range of depths in the forest. In addition, the embedded sensor network was depleted of snow as much as 4 weeks earlier than the snow pillow each year. Based on the February and April snow surveys, the embedded sensor network was able to capture the mean spatial snow depth and variability over the modeled 1-, 4-, and 16–km^2 grid (Figure 3) for the melt period, but overestimated the spatial mean for the accumulation period. In February, during the snow survey, the 8 operational snow depths sensors in the embedded sensor network had a spatial mean depth of 65 cm, which was within 5% of the 1-, 4-, and 16-km^2 mean modeled snow depth.

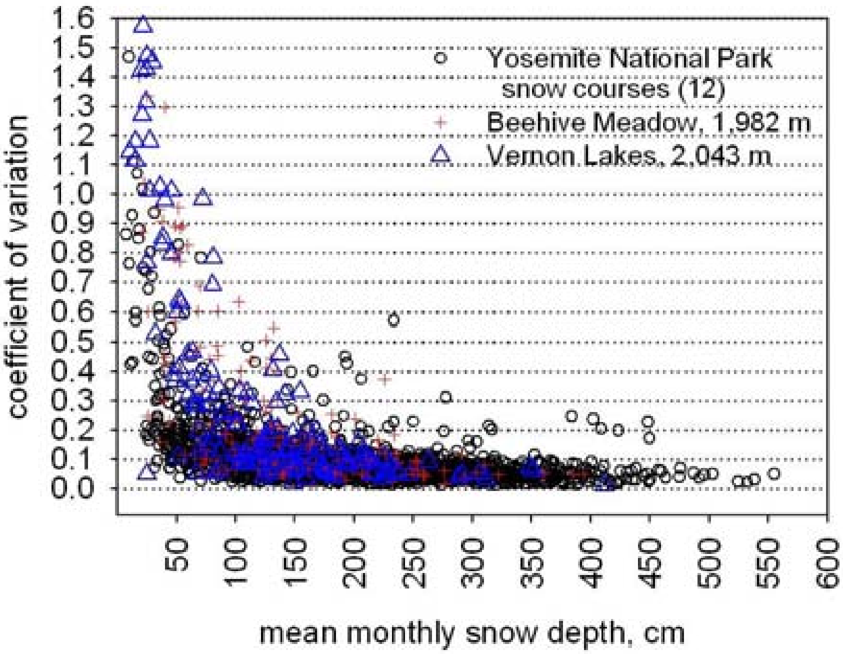

Figure 2. Historical mean April 1 snow depth and the coefficient of variation for each sample point along the transect within the snow course.

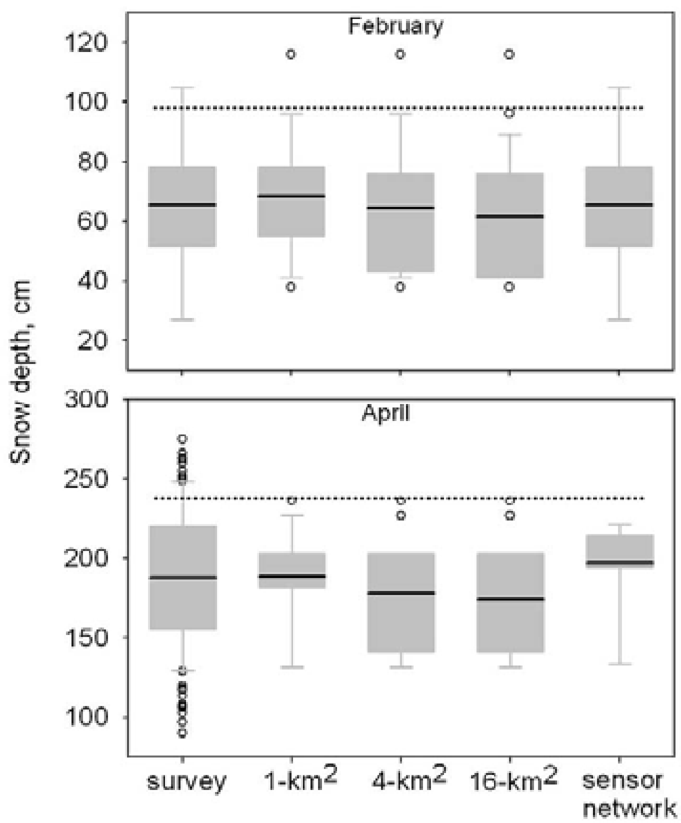

Figure 3. Snow distribution patterns from the snow survey, the 1-, 4-, and 16-km^2 modeled areas, and the embedded sensor network. The circles represent the outliers. The dotted line represents the snow pillow recorded at Gin Flat.

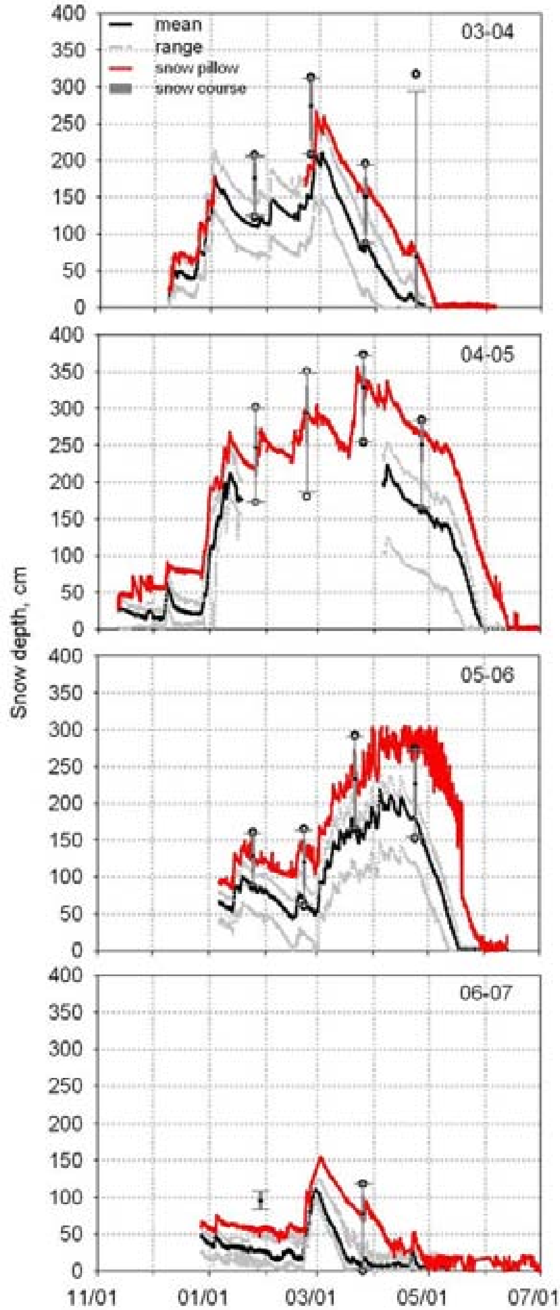

Figure 4. Hourly snow-depth measurements for ultra-sonic depth sensors, snow pillow data, and monthly snow course.

The CV was 0.33 for the embedded sensor network, indicating a slightly greater spread of snow depths than the modeled values of 0.28, 0.30.and 0.30 for the 1-, 4-, and 16 km^2, respectively, however the embedded sensor network was not able to capture the lower snow depths that are represented by the first quartile in the 4- and 16-km^2 modeled snow depths. In April, the embedded snow sensor network overestimated the mean spatial snow depth by 5% when compared to the 1-km^2 mean modeled snow depth, and 10% and 12% at the 4- and 16-km^2 modeled snow depths. The CV for the embedded sensor network was 0.13, indicating only a slightly lower of values than the modeled snow depth values of 0.16 and 0.18 for the 1-, 4-, and 16 km^2. However, the embedded sensor network was unable to capture the distribution of snow depths values as modeled over the 1-, 4-, and 16-km^2 study during the April accumulation period. The embedded sensor network does capture an observed value near the lowest modeled value for the both the 4- and 16 –km^2 area, but the embedded snow sensors are positively skewed toward higher snow depths, and more representative of the 1-km^2 modeled snow depths. It should be noted that the snow pillow and even the snow course measures 33% and 17% above the spatial mean as measured by the embedded sensor network (Figure 3).

DISCUSSION

Spatial Variability

Snow course measurements made late in the season after the April 1, or measurements taken during low snow years show more degree of variability across a snow course, with CV's > 0.30. The spatial variability at the snow course, as measured by the CV, is affected by the mean monthly snow depth. As the mean monthly snow depth declines, the spatial variability across the 10 sample points increases, as vegetation begins to influence the snow distribution patterns. The influences of vegetation are apparent once the mean monthly snow depth begins to fall below 100 cm, as the CV begins to increase exponentially, increasing above 0.50.

Overall, the analysis of the individual snow depths, from the snow course showed little deviation from the mean snow depth at all 14 snow courses. Using the CV as a measure of the variability, 90% of the CV's were <0.20 for snow courses above 2,100-m, and 70% of all measurements points fall within 10% of the spatial mean, indicating that the snow cover is homogenous in nature across the transects of these snow courses. Therefore, given the complex terrain surrounding the snow course, it becomes challenging to capture the spatial mean and the distribution patterns of snow, over terrain that is characterized with no slope, aspect, or any significant vegetation.

The extensive field surveys resulted in lower CV's, 0.39 and 0.41 and 0.20 and 0.27, for February and April, respectively, than the values reported for snow depth by Erickson et al. (2005), which ranged from 0.69 to 1.09 for the Green Lakes Valley in the Colorado Front Range, 0.33 to 0.63 reported by Elder et al. (1991) in the Emerald Lakes Basin in the Sierra Nevada, and Molotch and Bales (2005) in the headwaters of the Rio Grande in the San Juan Mountains of Colorado, which ranged form 0.07 to 0.96. However, this previous work was performed in alpine watersheds, above treeline, which were subjected to a greater redistribution of snow resulting from wind effects, which are not significant in the forested area surrounding Gin Flat. Erickson (2005) determined that wind had the largest effect of snow depth resulting in significant variability throughout the study area in Colorado.

Regression tree analysis was attempted to capture the independent variables that control snow distribution, and to develop relationships between snow depths and the independent variables. Work by Molotch (2005), Erxleben et al. (2002) and Elder et al. (1998) showed similar results in forest cover, as most of the large-scale variation surrounding the Gin Flat snow pillow was explained for both the accumulation and ablation season (R^2=0.65 and 0.55, respectively). An attempt was made to assess the small scale variation within each grid cell, which was possible due to the four measurements made within each cell, but several statistical tests proved that the variance of the measurements were not homogeneous: a Bartlett Test rejected the hypothesis of homogeneity, and a linear regression of the point variance against the spatial coordinates gave coefficients significantly different from zero. This small-scale variability was most likely driven by vegetation (<60% canopy density), due to canopy interception of snowfall, and vegetation-induced variability generated by out-going long wave radiation emissions. The regression tree analysis makes it apparent that the Gin Flat snow course, being located in an open grassy meadow, is not indicative of the surrounding variability of snow across the landscape and is not designed as measures of absolute snow depth, nor does it have the ability to yield snow depth estimates at the basin-scale (Dressler et al., 2006).

The design and installation of an embedded sensor network is not intended to replace existing long-term snow measurement sites, such as snow courses, snow pillows or SNOTEL, but to compliment these existing sites, with more intensive sampling to capture the variability across the complex landscape. Of particular difficulty is the task of identifying observational locations that are indicative of the inter-seasonal variability that exists between accumulation and ablation. Since topography is constant year to year snow tends to collect in similar areas, as well as melt in similar patterns, on an inter-annual basis, thus indicating that intense initial sampling is requisite to characterize the effects of the topographic parameters on snow distribution patterns (Erickson et al., 2005). Thus, strategic placement of an embedded network of snow depth measurements could improve the predictions of the spatial distribution patterns of snow without the need for intense extensive sampling.

Measurement Design

The extensive surveys coupled with snow depth modelling at the 1-, 4-, and 16-km^2 at Gin Flat, representative of accumulation and ablation provided guidance for optimal locations in order to capture the spatial mean and variability across the landscape. Similar work performed by Molotch and Bales (2005) identified optimal locations for these distinct snow regimes and recommended potential measurement locations for accumulation and ablation, but an embedded sensor network was not designed or installed to test this hypothesis. The binary regression tree analysis and snow depth modelling confirmed that the embedded sensor network was located in optimal locations to capture the snow distribution patterns for the accumulation and ablation season (Figure 5). Optimal locations to estimate the spatial mean were calculated for both the February and April snow surveys within the 1-, 4-, and 16- km² modeled area, and provided a performance metric for the embedded sensor network. The grid elements represent the lowest absolute deviance from the mean modeled snow depth, that is, the optimal locations which are represented in Figure 5 are within 10% of the modeled spatial mean. In February, representative of the ablation period, 34% of the grid cells were considered an optimal location in both the 1- and 4-km^2 modeled area, while only 19% of the grid cells are considered optimal locations for the spatial mean. The snow pillow and snow course site were not among those grid elements, and therefore not representative of the spatial mean during the ablation period. In April characteristic of the accumulation period, 61% of the grid cells were considered optimal within the 1-km^2 grid, while 19% and 6% of the areas were considered optimal for the 4- and 16-km^2 modeled area. During the accumulation period within the 1-km^2 modeled area, the snow pillow and snow course did fall within those modeled grid cells that were considered representative of the spatial mean for 1-km^2.

Based on these results and the placement of the embedded sensor network within and around these optimal locations, the network was able to capture the spatial variability and spatial mean for February (Figure 3). February's distribution patterns were driven by vegetation density and aspect, as long wave and short wave radiation emissions were the primary drivers of snowmelt, as indicated by the regression tree analysis. The location of each the 10 snow depth sensor provided adequate coverage and the 0.4 ha study site was characteristic of the physiographics over the 1-, 4-, and 16-km^2 modelled area. A comparisons of the snow depth measurements made by the embedded sensor network in February indicated that a single point measurement is a poor estimator of the spatial mean within that region considered as optimal, but 4 or more measurement points can reduce the uncertainty of capturing the spatial mean by >20%. This indicates that during the February ablation period, a network of 10 nodes were sufficient to capture the spatial mean and variability, with 4 to 5 nodes strategically placed at those optimal locations to capture the spatial mean.

April which was indicative the accumulation season, the embedded sensor network was able to capture the complete distribution of modelled snow distribution values. Though the distributed network were located in areas that were indicative of the spatial mean, it is apparent that the independent parameters that control the distribution patterns, such as vegetation (i.e. canopy density), which controls snow fall interception, and sublimation rates, as well as elevation, confounded the distribution patterns for April 2005. These results indicate the importance of canopy density, as verified by the binary regression tree analysis indicating that higher snow depths were located in areas with low canopy densities. The modelling results showed that the mean average snow depths increased with lower canopy densities, indicating that higher interception rates during accumulation resulted in lower snow depths due to the forest canopy. Therefore, higher snow depths where recorded at the embedded sensor network due to lower canopy densities (closures).

The results from April 2006 indicate that the current network needs to be repositioned, or additional sensors need to be added to include more dense forest cover, and possibly extend the network to capture a low elevation component. To get more complete coverage of these two-parameters, and to increase the capability of capturing the spatial variability, especially during accumulation, the embedded sensor network needs updating. This will require the elimination of the wires that currently connect the datalogger to the depth sensors, and restrict the maximum distance within the measurement array to 51 meters from the datalogger. Operational difficulties of the embedded sensor network occurred in 2004/2005 as the network was non-operational between January 15-April 1, missing both peak accumulation and the onset of ablation. This disruption was the result of rodents damaging the wires. Sensors 1, 7, and 8 were damaged beyond repair, and no reliable data was available. In subsequent years, 2005-2007, this problem was alleviated by installing the wiring system once the first permanent snow had insulated the ground, thus creating a protective layer between the ground and the wires. With the development of wireless "mote" networks, these sensing platforms will provide a robust and reliable method to extend a network beyond its traditional capabilities; by measuring critical terrain parameters that extend beyond the limitations of this current system, as well as eliminating damages resulting from extraneous environmental conditions (i.e. wildlife). Continued advancement of wireless distributed networks and increased flexibility in the management of strategic sensor placement will provide more complete and accurate coverage of distribution patterns that are distinctly unique for both the accumulation and ablation season.

In spring 2005 we installed and tested a second embedded sensor network located about 500 m northeast and consisting of 10 snow-depth sensors connected by wireless pods (Figure 1). These pods (Sensor Web) were advanced versions of those currently being developed and tested by a number of companies. This initial test focused on the technical aspects of placement and communications of this self-organizing array, as the snowpack was already well developed before the pods were installed and the snow disturbed during installation.

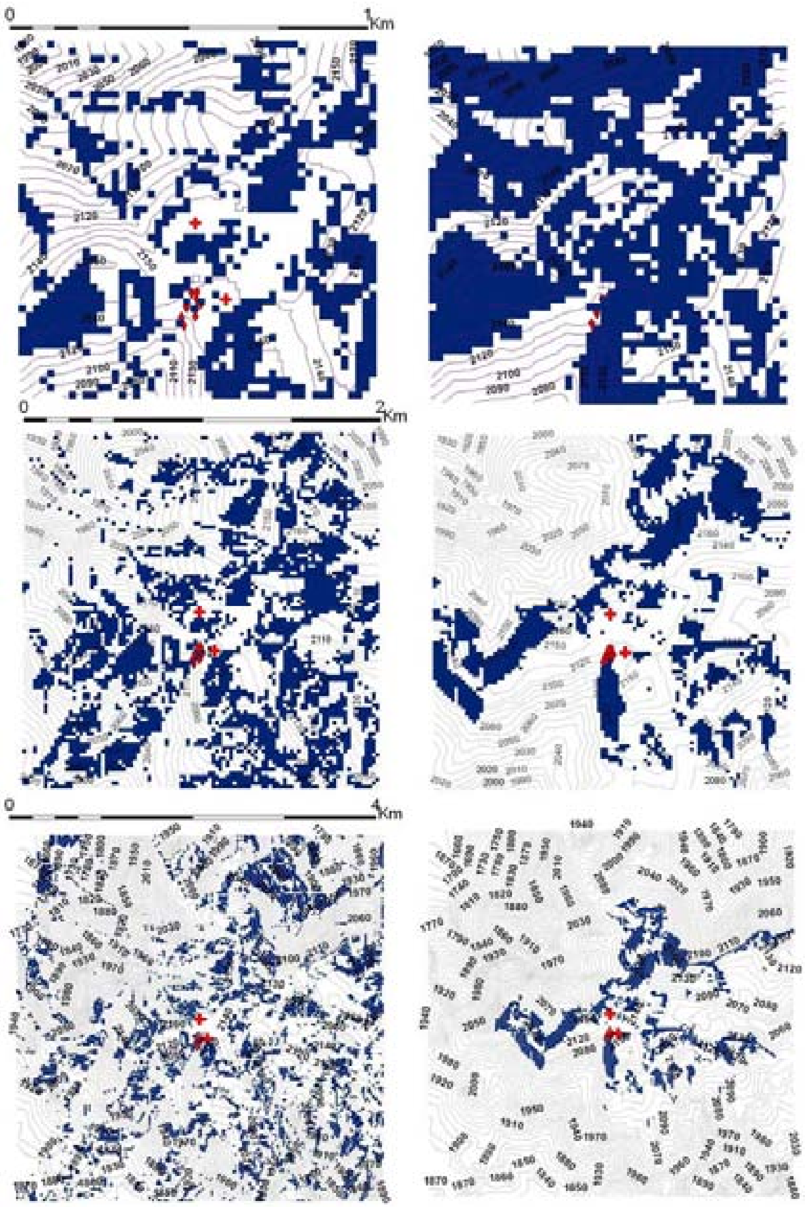

Figure 5. Optimal locations for measuring the mean spatial snow depth across the 1-, 4-, and 16 km^2 modeled snow depth area at Gin Flat. The left panels represent the ablation period in February, and the right panels represent the accumulation period in April. The diamonds represent the locations of the 10 nodes of the embedded sensor network while the crosses show the location of the snow pillow and snow course. The areas shaded in blue represent those areas with the values within 10% of the mean modeled snow depth.

CONCLUSIONS

At Gin Flat, neither individual snow course measurements nor the snow pillow, represent the km-scale spatial mean. As the snow course is not representative of the surrounding physiographic features, measurements within it are unable to resolve the spatial variability over distances greater than those observations. The snow course and snow pillow overestimated the mean spatial average by 20-30% across a 1-, 4-, and 16-km^2 modelled area. Snow courses are situated below timberline on flat or nearly flat terrain, and are placed in fetches that retain snow through most the winter season and during most winters, therefore overestimating the snowpack conditions specific to that elevation for the sub-basin. Individual point measurements that comprise the monthly snow course surveys in Yosemite, showed little variability within the snow course transects, as the coefficient of variation was <0.10.

Extensive snow surveys highlighted the physiographics that drive the snow distribution patterns, and verified that the embedded sensor network was located in optimal positions, indicative of the spatial mean and variability. Results demonstrated that the strategically placed acoustic snow depth sensors, sampling the independent variables controlling snow distribution and melt, can capture both the snow-distribution patterns and spatial mean during the ablation period. It can also capture the spatial mean for the accumulation period, though with greater uncertainty.

This prototype embedded sensor network also addresses the need to develop strategies to blend remotely sensed and ground-based data, to accurately define snow distribution across a basin. Currently, ground-based measurements are inadequate to provide the high spatial and temporal resolution, and verification of remotely sensed products. This prototype can be strategically replicated across a basin, providing coverage to under-sampled areas within a basin, including low-altitude ephemeral snow cover and high-altitude persistent snow cover. Continued advancement of these embedded networks, coupled with advancements in remote sensing, which provides additional spatially distributed parameters such as snow covered area, will not only improve basin-wide measurement of the seasonal snowcover, but will improve hydrologic monitoring, modelling, and study of the complex mountain system.

ACKNOWLEDGEMENTS

Support for this research was provided by NASA REASoN (NASA Grant NNG04GC52A) and National Science Foundation (NSF EAR 0610112) Observatory design, Additional support was provided by the University of California, Merced, Resources Management and Science Division at Yosemite National Park, and Kevin Delin at SensorWare Systems, Inc. We would also like to acknowledge the contributions of T. Bouffon, X. Meng, R. Dewit, S. Martin, N. Molotch, and L. Elits.

REFERENCES

Bales, R. C., N. P. Molotch, T. H. Painter, M. D. Dettinger, R. Rice, and J. Dozier. 2006. Mountain hydrology of the western United States. Water Resour. Res., 42, W08432, doi:10.1029/2005WR004387.

Blöschl, G. 1999. Scaling issues in snow hydrology. Hydrol. Processes, 13: 2149-2175, doi:10.1002/hyp, 847 p.

Brubaker, K. A., and M. Menoes. 2001. A technique to estimate snow depletion curves from time-series data using the beta distribution. Proc. East. Snow Conf., 58. pp. 343–346.

Carroll, T., D. Cline, G. Fall, A. Nilsson, L. Li, and A. Rost. 2001. NOHRSC operations and the simulation of snow cover properties for the coterminous U.S. Proc. West. Snow Conf., 69. pp. 1– 14.

Carroll, S.S., T.R. Carroll, and R.W. Poston. 1999. Spatial modeling and prediction of snow-water equivalent using ground-based, airborne, and satellite snow data. J. Geophys. Res.-Atmos., 104(D16): pp. 19623-19629.

Carroll S.S. and N. Cressie. 1996. A comparison of geostatisical methodologies used to estimate snow water equivalence. Water Resour. Bull. 32(2): 267-278.

Carroll, S. S., and T. R. Carroll. 1993 Increasing the precision of snow water equivalent estimates obtained from spatial modeling of airborne and ground-based snow data. Proc. East. Snow Conf., 50. pp. 83-87.

Cayan, D.R. 1996. Interannual climate variability and snowpack in the western United States. J. Clim., 9(5): 928-948.

Daly, S.F., R.E. Davis, E. Ochs, and T. Pangburn. 2000. An approach to spatially distributed snow modeling of the Sacramento and San Joaquin Basins, California. Hydrol. Processes, 14, 3257-3271, doi:10.1002/hyp 199 p.

Dressler, K.A., S.R. Fassnacht, and R.C. Bales (2006), A comparison of snow telemetry and snow course measurements in the Colorado River basin, J. Hydrometeorol., 7(4): 705-712.

Dozier, J. (1980), A clear-sky spectral solar radiation model for snow covered mountainous terrain, Water Resour. Res., 16, 709–718.

Elder, K., J. Dozier, and J. Michaelsen (1991), Snow accumulation and distribution in an alpine watershed, Water Resour. Res., 27, 1541 –1552.

Elder, K., W. Rosenthal, and R. Davis (1998), Estimating the spatial distribution of snow water equivalence in a montane watershed, Hydrol. Processes, 12, 1793– 1808. doi:10.1002/hyp.695.

Erickson, T. A., M.W. Williams, and A. Winstral (2005), Persistence of topographic controls on the spatial distribution of snow in rugged mountain terrain, Colorado, United States: Water Resour. Res., 41, W04014, doi:10.1029/2003WR002973.

Erxleben, J., K. Elder, and R. Davis (2002), Comparison of spatial interpolation methods for estimating snow distribution in the Colorado Rocky Mountains, Hydrol. Processes, 16, 3627– 3649, doi: 10.1002/hyp.1239.

Fassnacht, S.R., K.A. Dressler, and R.C. Bales (2003), Snow water equivalent interpolation for the Colorado River basin from snow telemetry (SNOTEL) data, Water Resour. Res., 39(8), 1208, doi:10.1029/2002WR001512.

Franz, K. J., H. C. Hartmann, S. Sorooshian, and R. Bales (2003), Verification of National Weather Service Ensemble Streamflow Predictions for Water Supply Forecasting in the Colorado River Basin, J. of Hydrometeol.,*4(6)*,1105-1118.

Ling, C., E.G. Josberger, and M. A.S. Thorndike (1995), Mesoscale variability of the upper Colorado River snowpack, Nordic Hydrology, 27, 313-322.

McGurk, B. J., T. J. Edens, and D. L. Azuma (1993), Predicting wilderness snow water equivalent with nonwilderness snow sensors, Water Resour. Bull., 29(1), 85-94.

Milly, P. C., D., Betancourt, J., Falkenmark, M., Hirsch, R. M., Kundzewicz, Z. W., Lettenmaier, D. P., and R.J. Stouffer (2008), Climate Change: Stationarity is dead: Whither Water Management? Science, 319, 573-574, doi:10.1126/science.1151915.

Molotch, N. P., T.H. Painter, R. Bales, and J. Dozier (2004), Incorporating remotely-sensed snow albedo into a spatially-distributed snowmelt model, Geophys. Res. Lett., 31, L03501, doi: 10.1029/2003GL019063.

Molotch, N. P., and R. C. Bales (2005), Scaling snow observations from the point to the grid element: Implications for observation network design, Water Resour. Res., 41, W11421, doi:10.1029/2005WR004229.

Mote, P.W., A.F. Hamlet, M.P. Clark, and D.P. Lettenmaier (2005), Declining mountain snowpack in western North America, Bull Am. Meteorol. Soc., 86(1): 39-49, doi:10.1175/BAMS-86-1-39.

Shafer, B. A., C. F. Leaf, and J. K. Marron (1979), Landsat derived snow cover as an input variable for snow melt runoff forecasting in south central Colorado, in *Satellite Hydrology*, edited by M. Deutsch et al., pp. 218– 224, Am. Water Resour. Assoc., Minneapolis, Minn.

Stewart, I.T., D.R. Cayan, and M.D. Dettinger (2005), Changes toward earlier streamflow timing across western North America, J. Clim., 18(8): 1136-1155.